frontiers in Materials

ORIGINAL RESEARCH
published: 30 June 2020
doi: 10.3389/fmats.2020.00191

Microstructure and Abrasive Wear Resistance of Mo_2C Doped Binderless Cemented Carbide

Xiuqi Zan[1,2], *Kaihua Shi*[2]*, *Kailin Dong*[2], *Jun Shu*[2] *and Jun Liao*[2]

[1] State Key Laboratory of Powder Metallurgy, Central South University, Changsha, China, [2] Zigong Cemented Carbide Corp, Ltd., Zigong, China

Binderless cemented carbide contains very little (<0.5 wt.%) or no metal binder and has an incomparable excellent wear resistance, corrosion resistance, excellent polishing, and oxidation resistance compare to traditional cemented carbide (Imasato et al., 1995). For now, many studies were focusing on the influence of Mo/Mo_2C on the microstructure and mechanical properties of traditional cemented carbide (Guo et al., 2008; Wang et al., 2010; Yu et al., 2015). However, to our knowledge, no report was found studying on Mo/Mo_2C added binderless cemented carbide. In this work, a series of binderless cemented carbides with diverse Mo_2C addition amounts (0–6 wt.%) were prepared by sintering and then hot isostatic pressing (HIP) at 2000°C under an isostatic pressure of 70 MPa. The microstructure and abrasive wear resistance of the obtained samples were systemically investigated. The grain size does not change with the increase of Mo_2C addition amount, while the abrasive wear resistance of the cemented carbide increases obviously. The data of the abrasive wear test show the wear volume loss of the cemented carbide reduces from 7.32 to 0.02 $cm^3/10^5r$ when the Mo_2C addition amount change from 0 to 6.0 wt.%. The superior abrasion resistance of samples with higher Mo_2C content and the smoother appearance of the worn surfaces with no definite pullout of grains compared with other samples were result from the forming of (W,Mo)C because of the intermixing between WC and Mo_2C caused by high temperature sintering.

Keywords: microstructure, binderless, cemented carbide, wear, Mo

Edited by:
Suryanarayana Challapalli, University of Central Florida, United States

Reviewed by:
Qiao Yanxin, Jiangsu University of Science and Technology, China
Dongchan Jang, Korea Advanced Institute of Science and Technology, South Korea

***Correspondence:**
Kaihua Shi
kaihua_shi@outlook.com

Specialty section:
This article was submitted to Mechanics of Materials, a section of the journal Frontiers in Materials

Received: *11 December 2019*
Accepted: *25 May 2020*
Published: *30 June 2020*

Citation:
Zan X, Shi K, Dong K, Shu J and Liao J (2020) Microstructure and Abrasive Wear Resistance of Mo_2C Doped Binderless Cemented Carbide. Front. Mater. 7:191. doi: 10.3389/fmats.2020.00191

INTRODUCTION

WC-Co cemented carbides have a wide range of industrial applications, being used in cutting tools, forming tools, impact resistant mold, and wear resistant parts due to their exceptionally high hardness, wear resistance, and good toughness (Shi et al., 2014; García et al., 2019). The properties of cemented carbides depend primarily on binding phase content and WC grain size. Typical WC-Co cemented carbides contain less than 30 wt% cobalt, and the WC grain size ranges from submicron levels to a few microns (Wu et al., 2016). The binding phase such as Co is good for fracture toughness and strength increase, but at the same time, it will also reduce the hardness, corrosion resistance, and wear resistance. What's more, because of the different thermal expansion coefficient compare to WC, cobalt may also cause thermal stress, which limits its application in high temperature and harsh conditions (Suzuki, 1986). Therefore, binderless cemented carbide has received growing research attention over recent years.

Binderless cemented carbide has excellent properties such as wear resistance and corrosion resistance etc. due to it's contains very little or no metal binder (Imasato et al., 1995). These advantages ensure it can be used in the production of milling cutter, reamer, high precision mold, water sand tube, fracturing nozzle, glass cutter knife, valves, water cannon, textiles, and tape cutter, etc. (Poetschke et al., 2012). Owing to the high melting point (2870°C) of the WC, a high sintering temperature up to 1700–2000°C should be adopted in order to get high density of non-bonded WC cemented carbide. At present, many sintering methods, such as discharge plasma sintering method, hot pressing method, pressure and pressureless sintering method etc. have been used to produce binderless WC cemented carbides (Zhang et al., 2009; Tsai et al., 2010; Kornaus et al., 2017). In recent years, many researches and exploration have been carried out in the field of binderless WC based cemented carbide, mainly focus on densifying and properties improvement. It was reported that the smaller the average particle size of WC powder is, the higher the hardness and bending strength are (Li and Liu, 2005). Furthermore, the presence of cobalt accelerated the sintering densification process of binderless WC cemented carbide, which also resulted in the obvious anisotropic non-continuous grain growth of WC grains (Zhang et al., 2011).

Mo and Mo_2C added traditional cemented carbides have been studied for many years because Mo has similar structure and properties to that of Yu et al. (2015) studied the effect of Mo content on the microstructure and properties of WC-8-(Fe-Co-Ni) cemented carbide. The results show that the increase of Mo content can reduce the solubility of WC in the liquid phase, so that the grain growth is refined and the hardness of the cemented carbide is significantly improved. Because of the solid solution strengthening of Mo, the bending strength of the cemented carbide is improved. The WC-8(Fe-Co-Ni) cemented carbide get the best comprehensive performance when the Mo content increased to 5 wt%. Wang et al. (2010) studied the effect of Mo addition on the microstructure and properties of WC-2Co cemented carbide. The results show that a small amount of Mo addition can refine WC grains, improve the relative density and hardness of the cemented carbide, but reduce the bending strength of the cemented carbide. When the amount of Mo addition is 2.4 wt%, the microstructure and comprehensive properties of the sample are the best. Guo et al. (2008) studied the effect of Mo_2C on the microstructure and properties of WC-Ti-Ni cemented carbide. The results show that Mo_2C is an effective inhibitor of grain growth. With the increase of Mo_2C addition (0→ 1.2 wt%), the grains of the alloy become finer, the hardness and bending strength increase. In addition, Mo_2C can improve the wettability of bonding phase Ni to WC. Surprisingly, there has been relatively little investigation of the effect of Mo/Mo_2C addition on the microstructure and properties of binderless cemented carbide.

In this work, a series of Non-bond cemented carbide with various Mo_2C doping amounts were prepared using traditional PM route. The effect of Mo_2C doping amount on microstructure and abrasive wear properties of the as-prepared samples were studied.

TABLE 1 | Compositions of WC-0.3Co-xMo_2C samples.

	WC(wt.%)	Co(wt.%)	Mo_2C(wt.%)
Sample 1	99.70	0.30	0
Sample 2	98.50	0.30	1.20
Sample 3	97.30	0.30	2.40
Sample 4	96.10	0.30	3.60
Sample 5	94.90	0.30	4.80
Sample 6	93.70	0.30	6.00

EXPERIMENTAL

In the research, three different analytical reagent grade powders (WC (≈0.4 μm), Mo_2C and Co) were mixed by ball milling to form initial powder mixture. The chemical compositions of the designed samples with different Mo_2C addition amount are given in **Table 1**. In this work, raw powders with a certain weight ratio were mixed in a rolling ball mill machine for 30 h at room temperature, using WC-6 wt%Co (ISO: K20) balls with a diameter of 6.35 mm as grinding media. The ball-to-powder mass ratio was 4:1 and the rotational speed was 80 rpm. Next, the slurry was dried in a 60°C oven for 60 min to obtain the powders for pressing. The powders were then pressed into green compacts with a radius of 25 ± 0.5 mm and rectangular specimens of 57 × 26 × 6 mm in dimension were also pressed for abrasive wear resistance tests.

All the samples were placed on a graphite tray and sintered in a HIP furnace (QIH-15, USA) with the maximum sintering temperature of 2000°C for a dwell time of 90 min. During the maximum sintering temperature, an isostatic pressure of 70 MPa was applied to the samples using Ar.

Microstructural features of the specimens as well as the compositional analysis of certain phases were examined by optical microscopy (Leica DMI 5000 M) and scanning electron microscopy (EVO-18) equipped with an X-Max-20 X-ray energy dispersive spectroscopy (EDS) system. A D/max2550pc X-ray diffractometer was utilized to obtain the X-ray diffraction (XRD) patterns of the as-prepared specimens.

The abrasive wear resistance of the cemented carbide was conducted under wet conditions with Al_2O_3 (particle size: 500–560 μm) and water as the abrasive media at room temperature (20 ± 2°C) using MLS-40 instrument (Shi et al., 2015). The test was done at a load of 196 N and rotation number of 5,000 r. The rotational speed was 120 r·min^{-1}.

RESULTS AND DISCUSSION

Microstructure

Figure 1 shows the XRD patterns of the WC-0.3Co-xMo_2C alloys after sintering. The peaks of the six group of samples are similar, which are identified as two main phases corresponding to WC and Mo_2C. However, the Bragg peaks for "WC" of the sintered samples tend to shift toward higher angles with increasing Mo_2C addition amount, as shown in XRD patterns (**Figures 1A,B**). This is mainly because "MoC" and WC have

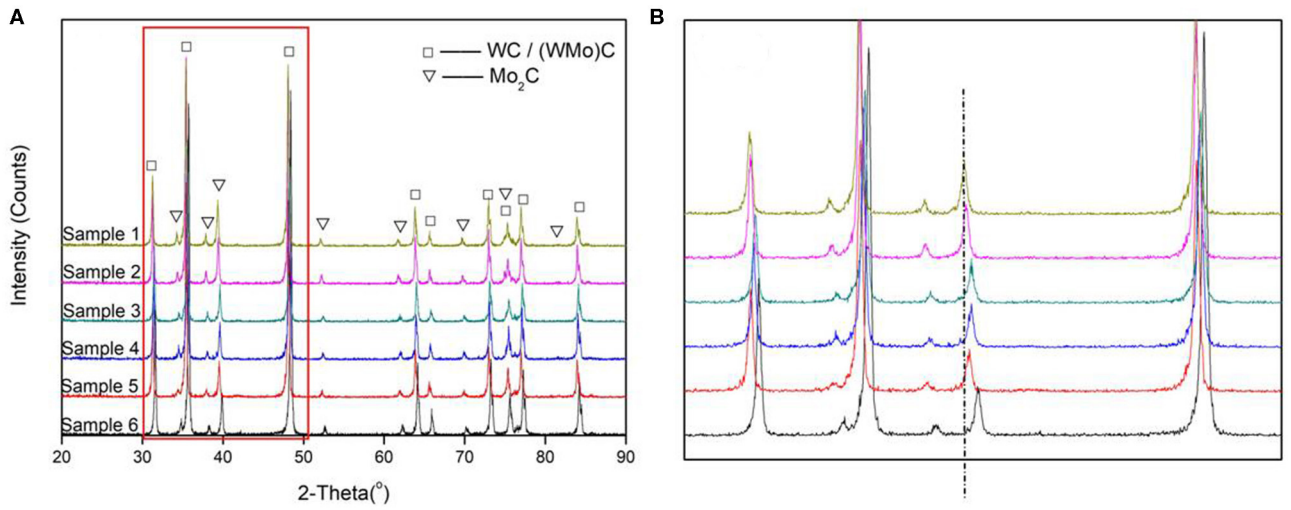

FIGURE 1 | XRD patterns of **(A)** WC-0.3Co-xMo_2C alloys after sintering and **(B)** region of interest in **Figure 2**.

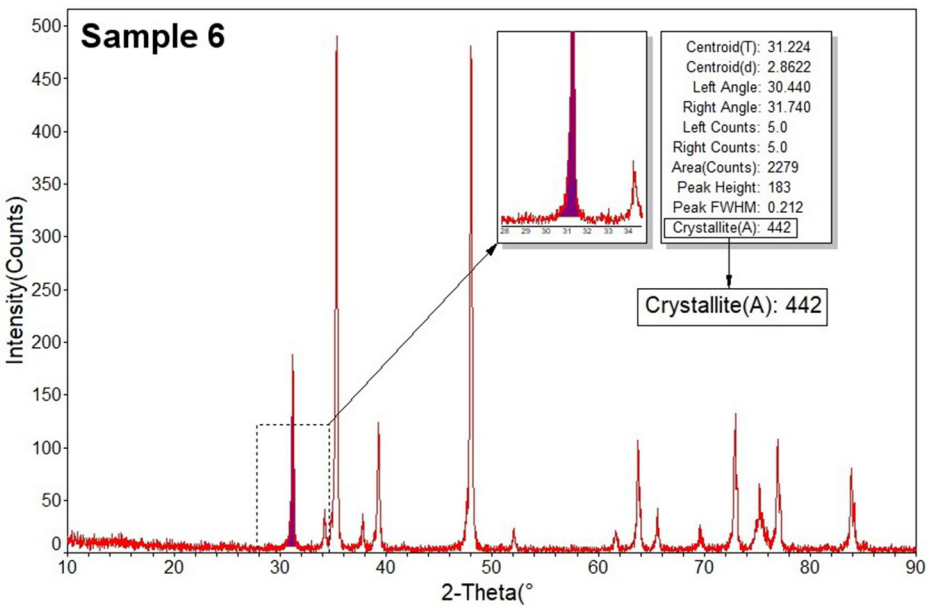

FIGURE 2 | XRD patterns of sample 6 with 6.0 wt.% Mo_2C content.

very similar crystallographic structures. A complete range of solid solution exists between WC and "MoC" below 1180°C (Shi et al., 2015). The sintering temperature used in this study is up to 2000°C. A possible reaction path for the formation of mixed WC-Mo_2C-C grains could be Mo_2C+C+WC→ (W,Mo)C (Rudy et al., 1978; Schwarz et al., 2016; Shi et al., 2017). The lattice parameter value "a" of "MoC" is 2.9030 Å, which is lower than that of WC (2.9063 Å). Thus, it seems reasonable that the shifting of "WC" peaks to higher angles is caused by the shrinking lattice.

The XRD results can also be used to evaluate the grain sizes of the samples. **Figure 2** shows the fitting of the peaks in low angle of sample 6, which gives us some information including the WC crystallite dimension. The crystallite WC of other samples was analyzed by this method and the results show that the crystallite WC of all samples is 452, 431, 440, 427, 455, and 442 Å, separately. It means that there is no significant difference between them.

Figures 3A–F shows the SEM images of the polished surfaces of the sintered samples after etching. The images were converted to binary images using a freeware image analysis Image-J (NIH, http://rsb.info.nih.gov/ij/) in order to observe the WC grains' boundaries. For binary images converting, the original images were first opened and convert to 8-bit files. Then threshold values

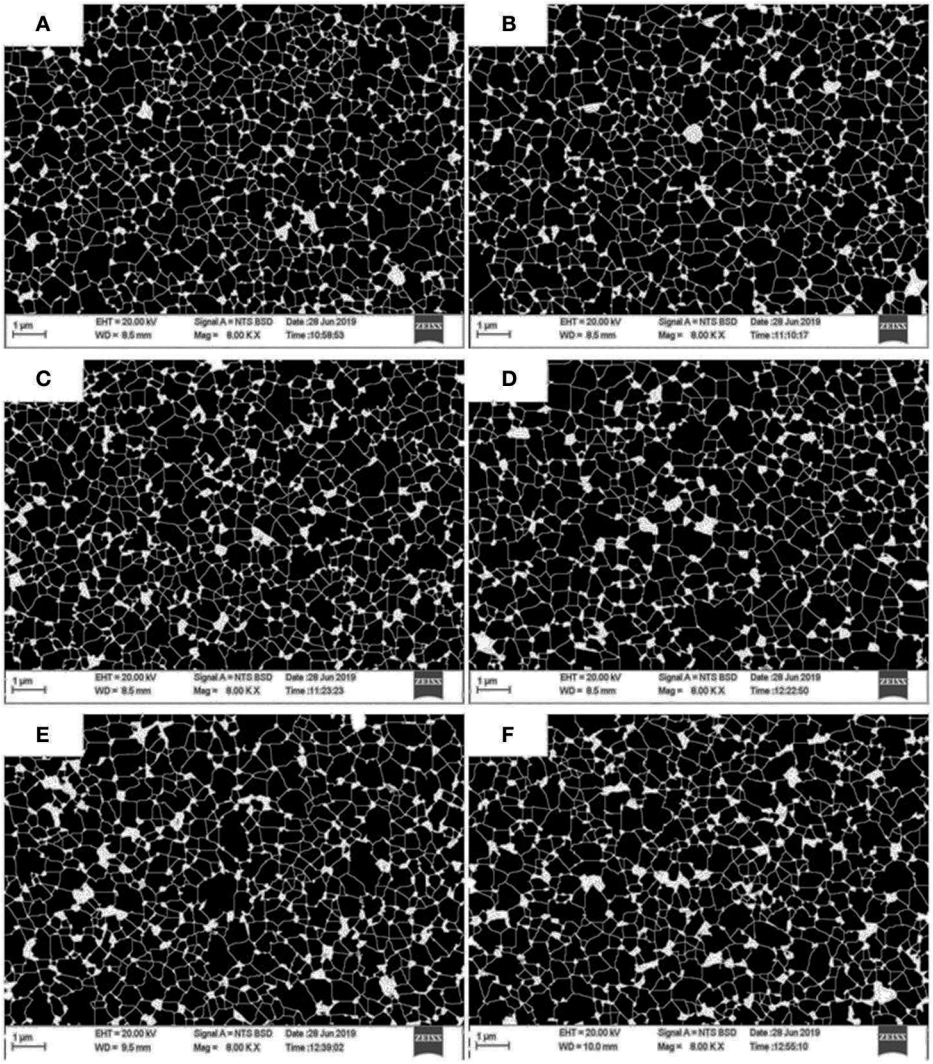

FIGURE 3 | Binary images of the alloys with different Mo_2C addition amount: **(A)** 0% Mo_2C; **(B)** 1.2% Mo_2C; **(C)** 2.4% Mo_2C; **(D)** 3.6% Mo_2C; **(E)** 4.8% Mo_2C; **(F)** 6.0% Mo_2C.

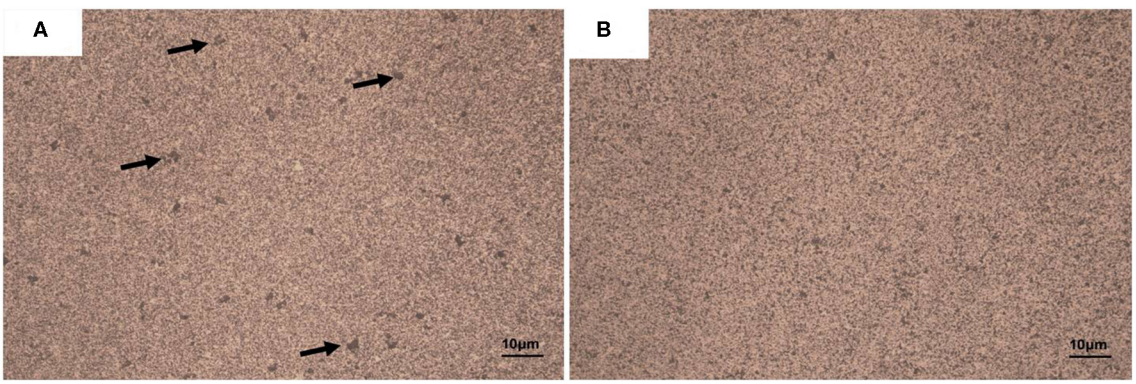

FIGURE 4 | The photomicrographs of the alloys with different Mo_2C addition amount: **(A)** 0% Mo_2C; **(B)** 6.0% Mo_2C.

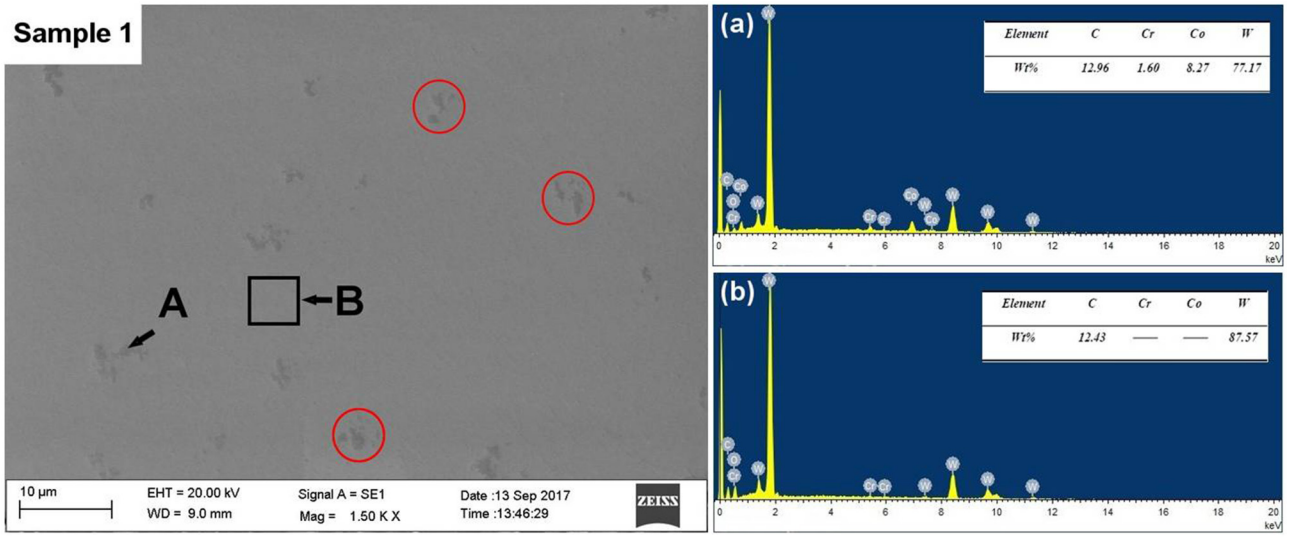

FIGURE 5 | SEM microstructure and EDX results of certain areas on the polished surface of sample 1: **(a)** Point A; **(b)** Area B.

were determined empirically by selecting a setting, which gave the most accurate binary image for analysis. Watershed was chosen for processing to get the final images with clear grain boundaries. As shown in the pictures, there is no significant difference of WC grains size between the samples with different Mo_2C content. This indicates that Mo_2C has little effect on WC grain growth in binderless cemented carbide under the adopted HIP sintering process parameters.

There are two theories about the effect of Mo_2C as a WC grain growth inhibitor. One is that Mo_2C acts a barrier to the WC growth because Mo_2C might precipitate in the WC grains interface. Therefore, it is difficult for WC grains to grow to incorporate those Mo_2C impurity atoms (Bosio et al., 2018). Nevertheless, according to the discussion about solid solution between molybdenum carbide and tungsten carbide earlier in this paper, it is reasonable that a reaction of mixed WC-Mo_2C-C grains exists. Therefore, this theory is not suitable for this study. The other theory is based on WC grain abnormal growth mechanism. Morton et al. (2005) reported that WC grain abnormal growth occurs during liquid phase sintering due to re-precipitations of the small WC dispersed in Co on the large solid WC grains (Ostwald ripening). The main driving force of the mentioned phenomenon is mainly the reduction in surface energy of the solid particles during sintering. Many reports (Kang et al., 2002; Morton et al., 2005; Fang et al., 2009; Zhao et al., 2015) believed that Mo_2C dissolves in binder phase can restrain the dissolution and re-precipitation of WC in binder phase during liquid phase sintering process, thus inhibit the individual growth of WC grains. If there is limit binder phase, the effect of Mo_2C on WC individual grain growth may be not significant, which is the case of this study.

Figures 4A,B show the photomicrographs of the sintered samples with 0 and 6.0 wt.% Mo_2C content, separately. Bright areas correspond to WC. Both of the alloys contain "dark areas" look like large pores (see arrows in **Figure 4A**). Meanwhile, the size and quantity of the "dark areas" decrease with the Mo_2C content increasing. In order to find out the morphology and chemical composition of the "dark areas," SEM and EDS are employed for the analysis of the chemical composition at fixed points on the polished surface of the alloy, and the results of sample 1 (other results of the samples are similar) are shown in **Figures 5a,b**.

From **Figure 5**, it can be ensured that the "dark areas" are not pores but liquid phase concentration. The EDX result of the "dark area" of sample 1 in **Figure 5** indicates that the area contains mainly Co and some elements dissolve in it. The size of the "dark areas" in **Figures 4A,B** decreases as Mo_2C content increasing, which means that the Co distribution becomes more uniform in the sample. This is because that after addition of Mo_2C, Mo dissolved in liquid Co and reduced wetting angle, thereby improving the wettability of Co relative to the WC phase (Balbino et al., 2017).

Abrasion Resistance

Figures 6, **7** show the images of the sample surface after abrasive wear testing, and their representative cross-section profile of worn surface, separately. According to **Figure 6**, the morphology of the wear scratches in sample 1∼4 are consist of many narrow grooves, while those of sample 5 and 6 are almost flat. It is obviously that the wear area of the samples decreasing against Mo_2C content increases. This change indicates that Mo_2C addition amount is a primary factor in the abrasive wear behavior of the samples. The morphology details of the wear scratches including width and depth of the samples are shown in cross-section profiles in **Figures 7A–F**. The difference between them is obvious in the images where the depth of the scratch of sample 1 with 0 wt.% Mo_2C addition is more than 0.5 mm, which is much deeper than that of other samples. For sample 5 with 4.8 wt.%

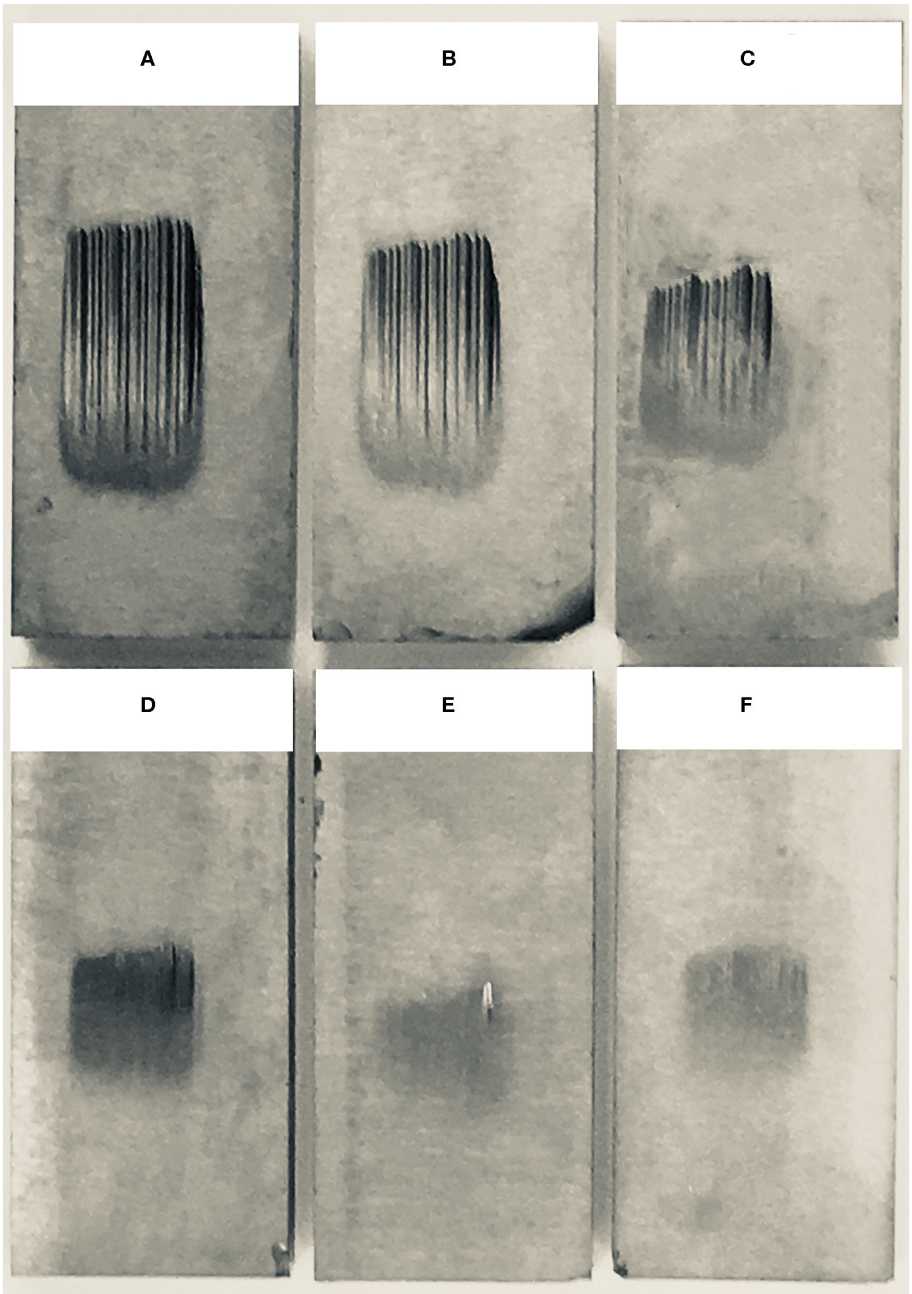

FIGURE 6 | Photos of the alloys with different Mo_2C addition amount after abrasive wear testing: **(A)** 0% Mo_2C; **(B)** 1.2% Mo_2C; **(C)** 2.4% Mo_2C; **(D)** 3.6% Mo_2C; **(E)** 4.8% Mo_2C; **(F)** 6.0% Mo_2C.

Mo_2C, the depth of scratch significantly decreases from 0.25 mm to ∼0.05 mm in comparison to sample 3 with 2.4 wt.% Mo_2C content. In sample 6 (**Figure 6F**), it can be seen that it is hard to obtain the cross-section profile because of the slight wear scratch result from the maximum Mo_2C addition amount (6.0 wt.%) in the sample.

The wear volume loss of different samples is shown in **Figure 8**. It can be seen in the picture that the wear volume tends to decrease with the Mo_2C content which is in accordance with the images in **Figures 6**, **7**. The wear volume loss decreases from 7.32 $cm^3/10^5 \cdot r$ for sample 1 to 0.04 $cm^3/10^5 \cdot r$ for sample 5 with 4.8 wt.% Mo_2C. However, the wear volume loss of the sample 6 containing 6.0 wt.% Mo_2C decreases slightly to 0.02 $cm^3/10^5 \cdot r$.

The SEM images of surface scratches of all the samples at low and high magnification are shown in **Figures 9A–F**. It is well-known that the wear resistance is usually determined in accordance with the wear mechanisms, which can be identified the worn surfaces analysis. Wear behavior in homogeneous

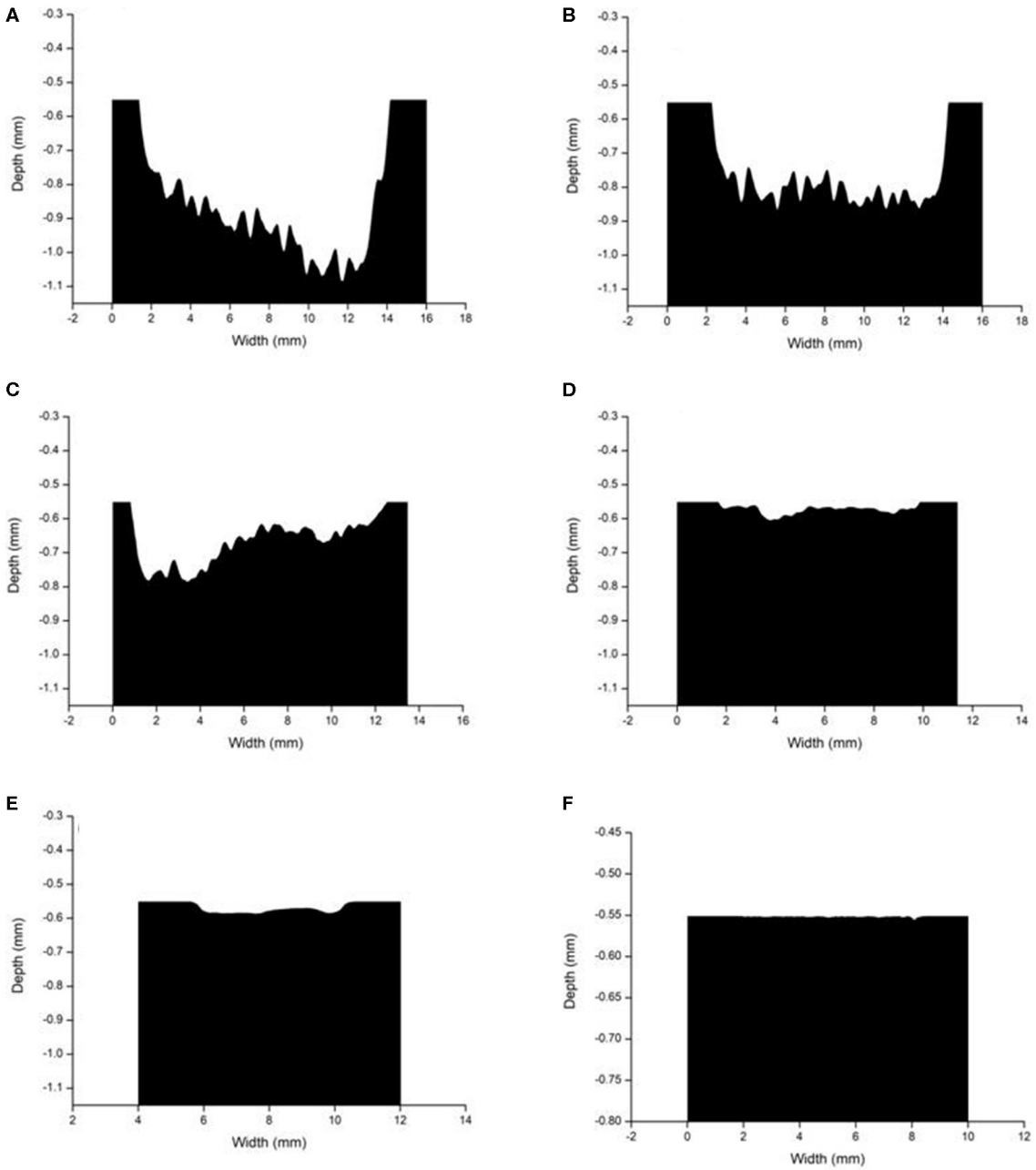

FIGURE 7 | Cross profiles of the samples' worn surfaces with different Mo_2C addition amount: **(A)** 0% Mo_2C; **(B)** 1.2% Mo_2C; **(C)** 2.4% Mo_2C; **(D)** 3.6% Mo_2C; **(E)** 4.8% Mo_2C; **(F)** 6.0% Mo_2C.

materials can be explained by adhesion, plastic deformation, delamination, plowing, microcracks, grain fragmentation and pull-out etc., and is dependent on their chemical and physical properties (Suh et al., 2008; Lee et al., 2010; Wang et al., 2010, 2018). In the abrasive wear testing process, several complex wear mechanisms may exist at the same time. **Figures 9A–D** shows the scratches images of samples with less Mo_2C content. Plowing and pullout of entire WC grains can be observed obviously in high magnification images in **Figure 9**. With Mo_2C content increasing from 4.8 to 6.0 wt.% in **Figures 9E,F**, the plowing and WC grain spalling gradually disappears. The worn surface presented a smooth wear track with no apparent damage in **Figures 9E,F**, which means that the wear behaviors of sample with 6.0 wt.% Mo_2C content is consistent with the mild wear regime, which explained little wear volume loss in **Figure 8**.

Mo_2C addition can improve the wettability of Co relative to the WC phase, strengthen grain boundaries and phase boundaries (Zhang et al., 2011), thus avoid grain fragmentation

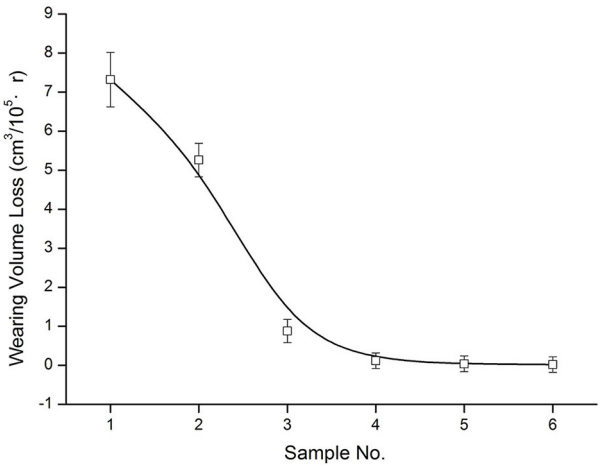

FIGURE 8 | Relationship of wearing volume loss against Mo_2C content:(1) 0% Mo_2C; (2) 1.2% Mo_2C; (3) 2.4% Mo_2C; (4) 3.6% Mo_2C; (5) 4.8% Mo_2C; (6) 6.0% Mo_2C.

and pull-out to some extent and enhance the wear resistance. According to the discussion of the foregoing, the liquid phase concentration in the sample decreases because Co distribution becomes more uniform as Mo_2C content increasing, thereby improving the binding force between WC and Co. However, it seems that this cannot be the only reason of the superior abrasion resistance of the samples with higher Mo_2C content because there is limit binder phase in all the samples.

It has been discussed earlier in this paper that the forming of (W,Mo)C due to the intermixing between Mo and W carbides when sintering at a high temperature is high due to the very similar crystallographic structures of WC-"MoC" and W_2C-Mo_2C (Shi et al., 2015). The superior abrasion resistance and smoother worn surfaces with less pullout of grains of samples with higher Mo_2C content are mainly result from the better grain boundaries due to the intermixing between Mo and W carbides (Engqvist et al., 2000). The wear volume loss results also show that binderless carbides with higher Mo_2C content have lower wear rate among the samples. According to previous study (Su et al., 2019), the bonding between the WC grains is the dominant

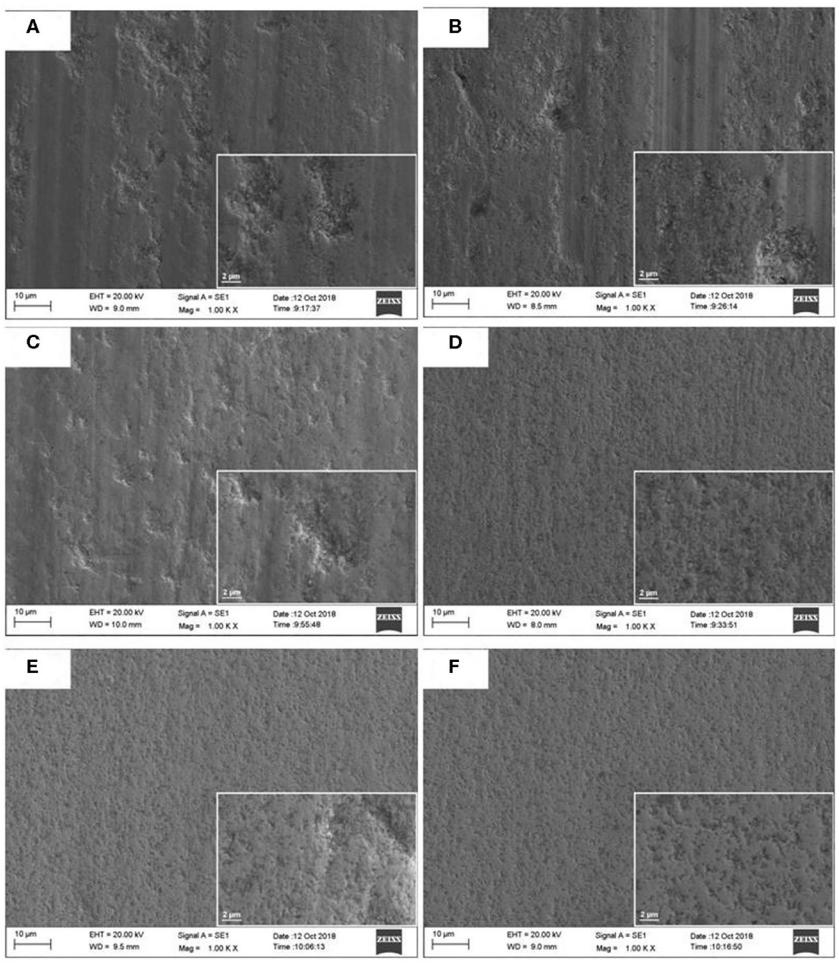

FIGURE 9 | SEM microstructures at low and high magnification of wear areas of the alloys with different Mo_2C addition amount (on the lower right of the figures are SEM images at 5000 times magnification): **(A)** 0% Mo_2C; **(B)** 1.2% Mo_2C; **(C)** 2.4% Mo_2C; **(D)** 3.6% Mo_2C; **(E)** 4.8% Mo_2C; **(F)** 6.0% Mo_2C.

factor of wear results of the binderless carbides. In this study, sample with 6.0 wt% Mo_2C is the best candidate due to its good WC-WC grains bonding.

CONCLUSIONS

In this paper, the effects of a small amount of Mo_2C on the microstructure and abrasion wear resistance properties of binderless cemented carbides were investigated. The results show that the addition of 1.2∼6.0 wt.% Mo_2C has little effect on WC grain growth because only 0.3% binder phase in the samples. The addition of Mo_2C could decrease the size of cobalt pool formation in the sample and promote the uniform distribution of binder phase. Moreover, the volume loss, cross-section profiles and the surface scratches show the abrasion resistances of the binderless cemented carbides with higher Mo_2C addition amount are superior to those of cemented carbides without or with less Mo_2C addition. This may result from the forming of (W,Mo)C due to the intermixing between WC and Mo_2C after sintering at a high temperature due to the very similar crystallographic structures of Mo and W carbides. In consequence, the cemented carbide has more wear-resistant because of the better grain boundaries caused by WC-"MoC" and W_2C-Mo_2C intermixing.

DATA AVAILABILITY STATEMENT

The raw data supporting the conclusions of this article will be made available by the authors, without undue reservation, to any qualified researcher.

AUTHOR CONTRIBUTIONS

KS, XZ, and KD were work together on the experiment. JS and JL gave help on the microstructure observation and properties testing. XZ and KS wrote this manuscript together. All authors contributed to the article and approved the submitted version.

REFERENCES

Balbino, N. A. N., Correa, E. O., Valeriano, L. C., and Amâncio, D. A. (2017). Microstructure and mechanical properties of 90WC-8Ni-2Mo_2C cemented carbide developed by conventional powder metallurgy. *Int. J. Refract. Metals Hard Mater.* 68, 49–53. doi: 10.1016/j.ijrmhm.2017.06.009

Bosio, F., Bassini, E., Oñate Salazar, C. G., Ugues, D., and Peila, D. (2018). The influence of microstructure on abrasive wear resistance of selected cemented carbide grades operating as cutting tools in dry and foam conditioned soil. *Wear* 394–395, 203–216. doi: 10.1016/j.wear.2017.11.002

Engqvist, H., Botton, G. A., Axe'n, N., and Hogmark, S. (2000). Microstructure and abrasive wear of binderless carbides. *J. Am. Ceram. Soc.* 83, 2491–2496. doi: 10.1111/j.1151-2916.2000.tb01580.x

Fang, Z. Z., Wang, X., Ryu, T., Hwang, K. S., and Sohn, H. Y. (2009). Synthesis, sintering, and mechanical properties of nanocrystalline cemented tungsten carbide e a review. *Int. J. Refract. Metals Hard Mater.* 27, 288–299. doi: 10.1016/j.ijrmhm.2008.07.011

García, J., Ciprés, V., C., Blomqvist, A., and Kaplan, B. (2019). Cemented carbide microstructures: a review. *Int. J. Refract. Metals Hard Mater.* 80, 40–68. doi: 10.1016/j.ijrmhm.2018.12.004

Guo, Z. X., Xiong, J., Yang, M., Song, X. Y., and Jiang, C. J. (2008). Effect of Mo_2C on the microstructure and properties of WC–TiC–Ni cemented carbide. *Int. J. Refract. Metals Hard Mater.* 26, 601–605. doi: 10.1016/j.ijrmhm.2008.01.007

Imasato, S., Tokumoto, K., and Kitada, T. (1995). Properties of urtra-fine grain binderless cemented carbide 'RCCFN'. *Int. J. Refract. Metals Hard Mater.* 13, 305–312. doi: 10.1016/0263-4368(95)92676-B

Kang, M. K., Kim, D. Y., and Hwang, N. M. (2002). Ostwald ripening kinetics of angular grains dispersed in a liquid phase by two-dimensional nucleation and abnormal grain growth. *J. Eur. Ceram. Soc.* 22, 603–612. doi: 10.1016/S0955-2219(01)00370-3

Kornaus, K., Raczka, M., Gubernat, A., and Zientara, D. (2017). Pressureless sintering of binderless tungsten carbide. *J. Eur. Ceram. Soc.* 37, 4567–4576. doi: 10.1016/j.jeurceramsoc.2017.06.008

Lee, C. W., Han, H. J., Yoon, J., Shin, M. C., and Kwun, S. I. (2010). A study on powder mixing for high fracture toughness and wear resistance of WC-Co-Cr coatings sprayed by HVOF. *Surf. Coat. Tech.* 204, 2223–2229. doi: 10.1016/j.surfcoat.2009.12.014

Li, R. Q., and Liu, T. M. (2005). Effects of processing parameters on the properties of Non-bond Cemented Carbide. *Cement. Carbide* 22, 23–26. doi: 10.3969/j.issn.1003-7292.2005.01.006

Morton, C. W., Wills, D. J., and Stjernberg, K. (2005). The temperature ranges for maximum effectiveness of grain growth inhibitors in WC-Co alloys. *Int. J. Refract. Metals Hard Mater.* 23, 287–293. doi: 10.1016/j.ijrmhm.2005.05.011

Poetschke, J., Richter, V., and Holke, R. (2012). Influence and effectivity of VC and Cr3C2 grain growth inhibitors on sintering of binderless tungsten carbide. *Int. J. Refract. Metals Hard Mater.* 31, 218–223. doi: 10.1016/j.ijrmhm.2011.11.006

Rudy, E., Kieffer, B. F., and Baroch, E. (1978). HfN coatings for cemented carbides and new hard-facing alloys on the basis (Mo,W)C–$(Mo,W)_2C$. *Planseeber Pulvermetall.* 26, 105–115.

Schwarz, V., Shi, K., and Lengauer, W. (2016). *Metallurgy and Properties of Mo-doped WC-Co and (W,Mo)C-Co Hardmetals*. Hamburg: WorldPM.

Shi, K., Schwarz, V., and Lengauer, W. (2017). "Preparation and properties of (W,Mo)C powders and (W,Mo)C-Co cemented carbides," in *19th Plansee Seminar* (Reutte).

Shi, K., Zhou, K., Li, Z., and Zan, X. (2014). Optimization of initial WC grain-size distribution in WC-6Ni cemented carbides. *J. Mater. Eng. Perform.* 23, 3222–3228. doi: 10.1007/s11665-014-1117-2

Shi, K., Zhou, K., Li, Z., Zan, X. Q., Dong, K. L., and Jiang, Q. (2015). Microstructure and properties of ultrafine WC–Co–VC cemented carbides with different Co contents. *Rare Metals*. doi: 10.1007/s12598-014-0424-y. [Epub ahead of print].

Su, Q. D., Zhu, S. G., Ding, H., Bai, Y. F., and Di, P. (2019). Comparison of the wear behaviors of advanced and conventional cemented tungsten carbides. *Int. J. Refract. Metals Hard Mater.* 79, 18–22. doi: 10.1016/j.ijrmhm.2018.10.019

Suh, M. S., Chae, Y. H., and Kim, S. S. (2008). Friction and wear behavior of structural ceramics sliding against zirconia. *Wear* 264, 800–806. doi: 10.1016/j.wear.2006.12.079

Suzuki, H. (1986). *Cemented Carbide and Sintered Hard Materials*. Tokyo: Maruzen Publishing Company.

Tsai, K. M., Hsieh, C. Y., and Lu, H. H. (2010). Sintering of binderless tungsten carbide. *Ceram. Int.* 36, 689–692. doi: 10.1016/j.ceramint.2009.10.017

Wang, H. B., Hou, C., Liu, X. M., Liu, X. W., and Song, X. Y. (2018). Wear resistance mechanisms of near-nanostructured WC-Co coatings. *Int. J. Refract. Metals Hard Mater.* 71, 122–128. doi: 10.1016/j.ijrmhm.2017.11.013

Wang, L. L., Li, H. Y., and Liu, N. (2010). Effect of Mo addition on microstructure and mechanical property of WC-Co-based carbides. *Rare Metals Cemen. Carb.* 38, 31–35. doi: 10.3969/j.issn.1004-0536.2010.02.008

Wu, C. C., Chang, S. H., Tang, T. P., Peng, K. Y., and Chang, W. C. (2016). Study on the properties of WC-10Co alloys adding Cr_3C_2 powder

via various vacuum sintering temperatures. *J. Alloys Compd.* 686, 810–815. doi: 10.1016/j.jallcom.2016.06.221

Yu, J. M., Feng, X., and Lu, L. (2015). Effect of molybdenum content on structure and properties of WC-8(Fe-Co-Ni) cemented carbide. *Jiangxi Sci.* 33, 888–893. doi: 10.13990/j.issn1001-3679.2015.06.023

Zhang, J., Zhang, G., Zhao, S., and Song, X. (2009). Binder-free WC bulk synthesized by spark plasma sintering. *J. Alloys Compd.* 479, 427–431. doi: 10.1016/j.jallcom.2008.12.151

Zhang, L., Chen, S., and Huang, F. J. (2011). Effects of small amount of cobalt addition on densification and WC grain growth during sintering of binderless cemented tungsten carbide. *Cement. Carbide* 28, 271–275. doi: 10.3969/j.issn.1003-7292.2011.05.001

Zhao, Z. Y., Liu, J. W., Tang, H. G., Ma, X. F., and Zhao, W. (2015). Effect of Mo addition on the microstructure and properties of WCeNieFe hard alloys. *J. Alloys Compd.* 646, 155–160. doi: 10.1016/j.jallcom.2015.05.277

Conflict of Interest: The authors declare that the research was conducted in the absence of any commercial or financial relationships that could be construed as a potential conflict of interest.